Analytical Solution for Power-Limited Optimal Rendezvous near an Elliptic Orbit

P. Sengupta[1] and S. R. Vadali[2]

Communicated by D. G. Hull

Abstract

This paper presents an analytical solution to the problem of optimal rendezvous using power-limited propulsion, for a spacecraft in an elliptic orbit in a gravitational field. The derivation of the result assumes small relative distances, but does not make any assumption on the eccentricity of the orbit, and does not require numerical integration. The results are generalized to include the possibility of different weights on the control effort for each axis (radial, along-track, and out-of-plane). When the weights on control efforts are unequal, several integrals are used whose solutions may be represented by infinite series in a small parameter dependent on the eccentricity. A methodology is introduced where the series can be extended trivially to as many terms as desired. Furthermore, for a given numerical tolerance, an upper bound on the number of terms required to represent the series is also obtained. When the weights are equal for all the three axes, the series representations are no longer necessary. The results can easily be used to design optimal feedback controls

[1]TEES Post-Doctoral Research Associate, Department of Aerospace Engineering, MS 3141, Texas A&M University, College Station, TX 77843-3141, E-mail: prasenjit@tamu.edu.

[2]Stewart & Stevenson - I Professor, Department of Aerospace Engineering, MS 3141, Texas A&M University, College Station, TX 77843-3141, E-mail: svadali@aero.tamu.edu.

for rendezvous maneuvers, or for generating initial guesses for two-point boundary value problems for numerical solutions to the nonlinear rendezvous problem.

Keywords

Optimal rendezvous, Power-Limited propulsion, Eccentric orbits, Tschauner-Hempel equations, Lambert W function

1. Introduction

The spacecraft rendezvous problem continues to be of great interest. In this problem, the requirement is one of the design of control algorithms to maneuver one spacecraft (designated as the chaser), to dock with another (designated as the target). The target may be empty; in this case the problem is one of relative orbit reconfiguration. However, the underlying theory is the same irrespective of the real or virtual target, and consequently, the entire class of relative maneuvers will be known as the rendezvous problem.

The optimal rendezvous problem refers to the design of algorithms, where a performance index, for example, elapsed time, or fuel required, is minimized. If the distance between the chaser and target is small when compared with the orbit size of the target, then analysis is considerably simplified, since the system of equations governing relative motion can be linearized using the target's orbit as a reference. The simplest linear model governing relative motion in a central field is given by Hill's equations (Ref. 1), which were used by Clohessy and Wiltshire (Ref. 2) for studying the rendezvous problem and are collectively known as the Hill-Clohessy-Wiltshire (HCW) model. These equations model relative motion in a local-vertical, local-horizontal (LVLH) Cartesian frame attached to and rotating with the target. The HCW model assumes a target in a circular orbit, in a central field. If the target orbit is eccentric, or if the gravitational field is perturbed, or if relative distance is not small, then

the HCW equations are no longer useful. The Tschauner-Hempel (TH) equations (Ref. 3) also constitute a sixth-order model, but are valid for all eccentricities. These equations have relative position scaled by the radial distance of the target satellite from the planet and use true anomaly of the target's orbit as the independent variable, instead of time. The TH equations are a nonautonomous system with periodic coefficients, and can be solved in terms of special integrals (Refs. 3–8).

Research on the rendezvous problem is well-represented in the literature. The general orbital transfer problem has been studied by several authors, too numerous to cite. In this paper, the focus is on linearized equations of relative motion, since the rendezvous problem implies that the distance between chaser and target is assumed small. Billik (Ref. 9) used a differential games approach to design optimal thruster programming laws for the HCW equations. Edelbaum (Ref. 10) formulated and solved the optimal rendezvous problem in terms of small orbital element differences. Gobetz (Ref. 11) also used a similar linearization in orbital element space, with the additional assumption of a near-circular target orbit, but used a nonsingular element set that extended the validity of the laws to those cases where eccentricity and inclination are zero - known singularities in the classical orbital element set. Alfriend and Kashiwagi (Ref. 12) formulated the open-loop, minimum-time rendezvous problem for elliptic orbits, using the TH equations. Jezewski and Stoolz (Ref. 13) formulated

the constant-thrust orbital transfer problem, by expressing the gravity field as a third-order polynomial in time by using two measurements of position and velocity and solving for the polynomial coefficients. Solutions to the continuous-thrust optimal rendezvous problem in a linearized gravity field, using the TH equations as a base, have been explored extensively by Refs. 4, 14, 15, among others. Although these references characterize the problem, they do not solve it. Primer vector theory was also used to analyze the problem of impulsive rendezvous, by Carter and Brient (Ref. 16). Inalhan *et al.* (Ref. 17) used linear programming to obtain velocity impulses optimally, for the establishment of satellite formations, using the TH equations. Euler (Ref. 18) approached the rendezvous problem by attempting to find an open-loop optimal control to the TH equations, for the standard low-thrust, limited-power quadratic cost function. However, a completely analytical solution could not be found, and results were obtained by restricting the equations to first order in eccentricity. Carter and Brient (Ref. 19) and Carter (Ref. 20) proposed a method to solve the problem posed by Euler (Ref. 18), but the procedure requires the numerical integration to evaluate a key matrix, for a complete solution. Coverstone-Carroll and Prussing (Ref. 21) solved the linear-quadratic regulator problem for circular orbits, using power-limited propulsion, and with control applied to both the target and chaser vehicles. Recent work by Zanon and Campbell (Ref. 22) developed an approximate solution for optimal open-loop, bounded-input control

for rendezvous near elliptic orbits, using Carter's solution (Ref. 6) to the TH equations as a basis. In this work, spline approximations were used for certain key integrals; however, closed-form solutions to these integrals were presented by Sengupta (Ref. 23).

In this paper, the fuel-optimal problem, for the linear system with quadratic cost (LQ problem) is solved by the use of several key integrals and functions of the eccentric anomaly. This is a natural consequence of the analytical solution to the TH equations. The more general power-limited cost function is first analyzed, where it is assumed that the weights on the control cost corresponding to the three axes of the rotating frame, are different. In this case, the appearance of several integrals whose closed-form analytical solutions are not yet known, is noted. However, series solutions to such integrals are developed, and it is shown that these solutions can be trivially extended to arbitrary order. Furthermore, an upper limit on the number of terms required for convergence within a desired tolerance is also obtained in a straightforward manner; and for practical purposes, the problem is solved completely. In the simpler, restricted case, where the in-plane weights are equal to each other (but not necessarily equal to the out-of-plane gain), no such integrals appear, and a closed-form, analytical solution is obtained to this problem.

The analysis in this paper is summarized as follows: the system model is first presented, and the optimal control problem is posed. The development of the analytical feedback control

law is then presented, followed by numerical examples to demonstrate its efficacy.

2. Relative Motion Equations

The relative motion equations are defined in the rotating Cartesian, LVLH frame attached to the target. This frame has basis vectors $\{i_r \quad i_\theta \quad i_h\}$, with i_r lying along the radius vector from the Earth's center to the satellite, i_h coinciding with the normal to the orbital plane of the target satellite, and $i_\theta = i_h \times i_r$. Let $\rho = xi_r + yi_\theta + zi_h$ denote the relative position vector of the chaser, with x, y, and z denoting the displacement along the radial, along-track, and out-of-plane directions, respectively, that have been scaled by the radial distance of the target from the Earth. The TH equations for rendezvous near a Keplerian elliptic orbit with arbitrary eccentricity $0 < e < 1$, can be written in the following state-space representation:

$$x' = A(f)x + B(f)u, \tag{1}$$

where $x \in X \subset \mathbb{R}^6$, $u \in U \subset \mathbb{R}^3$, $A : \mathbb{R}_{\geq 0} \to \mathbb{R}^{6\times 6}$, $B : \mathbb{R}_{\geq 0} \to \mathbb{R}^{6\times 3}$, and the following hold:

$$x = \left\{ \begin{array}{c} \rho \\ \rho' \end{array} \right\} = \{x \quad y \quad z \quad x' \quad y' \quad z'\}^\top, \quad B(f) = \frac{1}{(1+e\cos f)^3} \left[\begin{array}{c} \mathbb{O}_3 \\ \mathbb{1}_3 \end{array} \right],$$
$$A(f) = \left[\begin{array}{cc} \mathbb{O}_3 & \mathbb{1}_3 \\ \widetilde{A}(f) & \Omega \end{array} \right], \quad \widetilde{A}(f) = \left[\begin{array}{ccc} 3/(1+e\cos f) & 0 & 0 \\ 0 & 0 & 0 \\ 0 & 0 & -1 \end{array} \right], \quad \Omega = \left[\begin{array}{ccc} 0 & 2 & 0 \\ -2 & 0 & 0 \\ 0 & 0 & 0 \end{array} \right] \tag{2}$$

In the above, $(')$ denotes a derivative with respect to the true anomaly of the target, f, and $\mathbb{O}_3$ and $\mathbb{1}_3$ denote the 3×3 zero and identity matrices, respectively. The case $e = 0$,

corresponding to a target in a circular orbit, is avoided because the true anomaly is no longer defined in this case. This singularity may be removed by the use of nonsingular orbital elements, at the cost of more complicated expressions. This approach has not been explored here since a considerable amount of literature has been devoted to rendezvous near a circular orbit.

It should be noted that the dimensional control acceleration u_{appl} is obtained by the transformation $u_{\text{appl}} = (\mu/p^2)u$ where the semiparameter $p = a(1 - e^2)$.

The unforced TH equations can be solved (Ref. 3), by using a special integral, known as Lawden's integral (Ref. 8), which is expressed in terms of the eccentric anomaly, E. The eccentric and true anomalies are related by the following equation (Ref. 24):

$$\tan\frac{f}{2} = \sqrt{\frac{1+e}{1-e}}\tan\frac{E}{2}. \tag{3}$$

The special integral may be reformulated as shown in Refs. 4–7 to remove several artificial singularities. In this paper, the approach as shown in Ref. 7 is considered, to yield the following solution to the unforced TH equations:

$$\begin{aligned} x(f) = {} & c_1\cos f\,(1+e\cos f) + c_2\sin f\,(1+e\cos f) \\ & + \frac{2c_3}{\eta^2}\left[1 - \frac{3e}{2\eta^3}\sin f\,(1+e\cos f)\,k(f)\right], \end{aligned} \tag{4a}$$

$$y(f) = -c_1 \sin f\,(2 + e\cos f) + c_2 \cos f\,(2 + e\cos f)$$

$$-\frac{3c_3}{\eta^5}(1 + e\cos f)^2\, k(f) + c_4, \tag{4b}$$

$$z(f) = c_5 \cos f + c_6 \sin f, \tag{4c}$$

where $\eta = \sqrt{1 - e^2}$. The generalized relative velocity components can be obtained by taking the derivative of (4) with respect to f, resulting in the following expressions:

$$\begin{aligned} x'(f) &= -c_1(\sin f + e\sin 2f) + c_2(\cos f + e\cos 2f) \\ &\quad -\frac{3ec_3}{\eta^2}\left[\frac{\sin f}{(1 + e\cos f)} + \frac{1}{\eta^3}(\cos f + e\cos 2f)\, k(f)\right], \qquad (5a) \\ y'(f) &= -c_1(2\cos f + e\cos 2f) - c_2(2\sin f + e\sin 2f) \\ &\quad -\frac{3c_3}{\eta^2}\left[1 - \frac{e}{\eta^3}(2\sin f + e\sin 2f)\, k(f)\right], \qquad (5b) \\ z'(f) &= -c_5 \sin f + c_6 \cos f. \qquad (5c) \end{aligned}$$

In (4) and (5), the function $k(f)$ is obtained from Kepler's equation (Ref. 24), which can either be represented in integral form using the true anomaly, or the eccentric anomaly, or in terms of elapsed time Δt since epoch as shown below:

$$k(f) = \int_{f_0}^{f} \frac{\eta^3}{(1 + e\cos f)^2}\, df = (E - e\sin E) - (E_0 - e\sin E_0) = l - l_0 = n\,\Delta t. \tag{6}$$

In (6), $n = \sqrt{\mu/a^3}$ is the mean motion of the target's orbit, and l is the mean anomaly. Consequently, the use of $k(f)$ conveniently allows elapsed time from epoch, to appear in

the solution to the TH equations. It may be noted that the dimensional, unscaled state vector composed of relative position and velocity variables, can be obtained by multiplying the vector $\{x\ y\ z\ x'\ y'\ z'\}^\top$ by the following matrix:

$$\begin{bmatrix} p/(1+e\cos f)\,\mathbb{1}_3 & \mathbb{O}_3 \\ \sqrt{(\mu/p)}\,e\sin f\,\mathbb{1}_3 & \sqrt{(\mu/p)}\,(1+e\cos f)\,\mathbb{1}_3 \end{bmatrix}. \tag{7}$$

It is clear that the states at any value of true anomaly can be written in the form $x = L(f)c$ where $c = \{c_1 \cdots c_6\}^\top$, and the (j,k)th entry of L is the term with c_k as a coefficient, in the expression for the jth component of the state vector. In particular, let the initial conditions be denoted by $x_0 = \{x_0\ y_0\ z_0\ x_0'\ y_0'\ z_0'\}^\top$, specified at arbitrary initial true anomaly f_0. It can be shown that $\det L = 1$, and if M denotes the inverse of L, then $M = \text{adjoint}\, L$. It follows that $c = M(f_0)x_0$, where:

$$\begin{aligned} c_1 &= -\frac{3}{\eta^2}(e+\cos f_0)x_0 - \frac{1}{\eta^2}\sin f_0\,(1+e\cos f_0)x_0' \\ &\quad -\frac{1}{\eta^2}(2\cos f_0 + e + e\cos^2 f_0)y_0', \end{aligned} \tag{8a}$$

$$\begin{aligned} c_2 &= -\frac{3}{\eta^2}\frac{\sin f_0(1+e\cos f_0+e^2)}{(1+e\cos f_0)}x_0 + \frac{1}{\eta^2}(\cos f_0 - 2e + e\cos^2 f_0)x_0' \\ &\quad -\frac{1}{\eta^2}\sin f_0(2+e\cos f_0)y_0', \end{aligned} \tag{8b}$$

$$c_3 = (2+3e\cos f_0+e^2)\,x_0 + e\sin f_0\,(1+e\cos f_0)\,x_0' + (1+e\cos f_0)^2\,y_0', \tag{8c}$$

$$c_4 = -\frac{1}{\eta^2}(2+e\cos f_0)\left[\frac{3e\sin f_0}{(1+e\cos f_0)}x_0 + (1-e\cos f_0)x_0' + e\sin f_0 y_0'\right] + y_0, \tag{8d}$$

$$c_5 = \cos f_0\, z_0 - \sin f_0\, z_0', \tag{8e}$$

$$c_6 = \sin f_0\, z_0 + \cos f_0\, z_0'. \tag{8f}$$

As shown by Yamanaka and Ankersen (Ref. 7), the state transition matrix (STM) for the unforced TH equations is easily formulated by noting that

$$x = L(f)\, M(f_0)\, x_0 = \Phi_{xx}(f, f_0)\, x_0. \tag{9}$$

Other examples of STMs are provided in Ref. 6, 25–27. The STM derived in Ref. 26, although explicit in time, is valid for low eccentricities of the target's orbit. The STM for motion perturbed by Earth oblateness effects was derived in Ref. 27, and is identical to that in Ref. 25 if oblateness effects are ignored. This paper uses a formulation similar to Ref. 7 due to the use of relative position coordinates that are scaled by the radius of the target's orbit.

3. Cost Function for the Minimum-Fuel Problem

Depending on the requirements of the mission, different cost functions may be employed to pose the optimal control problem. For example, Alfriend and Kashiwagi (Ref. 12) formulated the open-loop, minimum-time rendezvous problem for elliptic orbits, using the TH equations. The fuel cost for engines using power-limited propulsion $\mathcal{J}_{\text{fuel}}$ is proportional to

the integral of the 2-norm of the control over time, and is given by (Refs. 28, 29):

$$\mathcal{J}_{\text{fuel}} \propto \int_0^T u^\top u \, dt \tag{10}$$

where t is the time, and T is the specified final time. However the cost function that is used for minimization in this paper, is of a more general form, given by:

$$\mathcal{J} \propto \int_0^T u^\top R u \, dt \tag{11}$$

The matrix $R \in \mathbb{R}^{3\times 3} > 0$ is a weight matrix, and it is usually sufficient to select $R = \text{diag}\{R_1, R_2, R_3\}$. When $R_1 = R_2 = R_3$, $\mathcal{J}$ is proportional to the fuel cost. The inclusion of this matrix in the cost function allows for better tuning when two or more thrusters are used, and one thruster is required to fire preferentially over the others. For example, control effort in the radial direction may not be efficient in some cases, as was demonstrated by Starin *et al.* (Ref. 30) for formation flight maneuvers near circular orbits. The radial control effort can be penalized by selecting the associated weight appropriately. Euler (Ref. 18) and Carter (Ref. 20) analyzed the optimal control problem with identical weights, although Ref. 18 also has shown that the system is controllable with no radial thrust, for all three axes.

To ensure consistency with the formulation of the dynamical equations, it is necessary to change the independent variable in (11) from time, t, to the true anomaly, f. This introduces an additional factor of $(1+e\cos f)^2$ in the denominator, as can be observed from (6). Without

loss of generality, the following cost function is used for power-limited propulsion:

$$\mathcal{J} = \frac{1}{2}\int_{f_0}^{f_T} \frac{u^\top R u}{(1+e\cos f)^2}\, df, \tag{12}$$

where f_0 and f_T are the known true anomaly values of the target, corresponding to epoch and final time. It will be shown in this paper that when $R_1 \neq R_2$, the development of a completely analytical solution is hindered by the appearance of some integrals whose closed-form solution is not yet known. This is a consequence of the appearance of $(1+e\cos f)^2$ in the denominator of (12). This inconvenience can be avoided by choosing a periodic gain matrix R, that cancels such terms. Although the control law resulting from this approach is not strictly power-limited fuel-optimal, it is still an optimal law, and has the additional advantage of penalizing the use of control near the periapsis of the orbit. Although the difference in the cost resulting from the use of the different laws is not negligible for moderate or high eccentricities, nonlinear effects in such studies will dominate (Ref. 31), and the application of linearized analysis is limited in scope.

4. Optimal Control Problem

For the system with dynamical equations governed by (1), and with a cost function (12), it can be shown that the necessary conditions for optimality (Ref. 32) yield the following

conditions for the control u and costates $\lambda \in \mathbb{R}^6$:

$$\lambda' = -A^\top(f)\,\lambda, \tag{13a}$$

$$u = -\widetilde{R}^{-1}(f)\,B^\top(f)\,\lambda, \tag{13b}$$

where,

$$\widetilde{R}(f) = \frac{1}{(1+e\cos f)^2} R. \tag{14}$$

For the augmented linear system comprising states and costates, the values of x and λ at any time are given by the STM Φ. Consequently, the initial values of λ can be found by the following:

$$\begin{aligned}
&\left\{ \begin{array}{c} x' \\ \lambda' \end{array} \right\} = \left[\begin{array}{cc} A(f) & -B(f)\,\widetilde{R}^{-1}(f)\,B^\top(f) \\ \mathbb{O}_6 & -A^\top(f) \end{array} \right] \left\{ \begin{array}{c} x \\ \lambda \end{array} \right\} \\
\Rightarrow \quad &\left\{ \begin{array}{c} x(f) \\ \lambda(f) \end{array} \right\} = \Phi(f, f_0) \left\{ \begin{array}{c} x(f_0) \\ \lambda(f_0) \end{array} \right\}, \qquad (15a) \\
&\Phi = \left[\begin{array}{cc} \Phi_{xx} & \Phi_{x\lambda} \\ \Phi_{\lambda x} & \Phi_{\lambda\lambda} \end{array} \right] \Rightarrow \lambda_0 = \Phi_{x\lambda}^{-1}(f_T, f_0) x_T - \Phi_{x\lambda}^{-1}(f_T, f_0)\Phi_{xx}(f_T, f_0)\,x_0. \qquad (15b)
\end{aligned}$$

Thus, the LQ problem can be solved if Φ_{xx}, $\Phi_{\lambda\lambda}$, $\Phi_{x\lambda}$ are known. Of these, Φ_{xx} is given by (9). The STM for the costates (Ref. 20) can be obtained by observing that the Hamiltonian system comprising x and λ leads to a state transition matrix that is symplectic in nature. If $\Im$ denotes the matrix of appropriate order that is analogous to the imaginary number

$\imath = \sqrt{-1}$, (15) implies that $\Phi \Im \Phi^\top = \Im$ or

$$\begin{bmatrix} \Phi_{xx} & \Phi_{x\lambda} \\ \Phi_{\lambda x} & \Phi_{\lambda\lambda} \end{bmatrix} \begin{bmatrix} \mathbb{O}_6 & \mathbb{1}_6 \\ -\mathbb{1}_6 & \mathbb{O}_6 \end{bmatrix} \begin{bmatrix} \Phi_{xx}^\top & \Phi_{\lambda x}^\top \\ \Phi_{x\lambda}^\top & \Phi_{\lambda\lambda}^\top \end{bmatrix} = \begin{bmatrix} \mathbb{O}_6 & \mathbb{1}_6 \\ -\mathbb{1}_6 & \mathbb{O}_6 \end{bmatrix}. \tag{16}$$

Resolving the matrix multiplication, and comparing the block matrices on both sides leads to four equations, one of which is

$$\Phi_{xx}\Phi_{\lambda\lambda}^\top - \Phi_{x\lambda}\Phi_{\lambda x}^\top = \mathbb{1}_6. \tag{17}$$

However, if x is not present in the cost function (as is the case considered here), λ does not depend on x, and $\Phi_{\lambda x} = \mathbb{O}_6$. It follows that

$$\Phi_{\lambda\lambda}(f, f_0) = \left[\Phi_{xx}^\top(f, f_0)\right]^{-1} = M^\top(f) L^\top(f_0). \tag{18}$$

From (18) and (13b), the solution to the forced system corresponding to (1), is:

$$x = \Phi_{xx}(f, f_0)x_0 - \int_{f_0}^{f} \Phi_{xx}(f, s)\, B(s)\, \widetilde{R}^{-1}(s)\, B^\top(s)\, \Phi_{\lambda\lambda}(s, f_0)\, \lambda_0\, ds \tag{19}$$

$$= \Phi_{xx}(f, f_0)x_0 + \Phi_{x\lambda}(f, f_0)\lambda_0. \tag{20}$$

The cross-component matrix $\Phi_{x\lambda}$ can be obtained by comparing (19) and (20) and is given by

$$\Phi_{x\lambda}(f, f_0) = -\int_{f_0}^{f} \Phi_{xx}(f, s)\, B(s)\, \widetilde{R}^{-1}(s)\, B^\top(s)\, \Phi_{\lambda\lambda}(s, f_0)\, ds$$

$$= -L(f)\left(\int_{f_0}^{f} M(s)\,B(s)\,\widetilde{R}^{-1}(s)\,B^{\top}(s)\,M^{\top}(s)\,ds\right)L^{\top}(f_0) \tag{21}$$

$$= -L(f)\,[N(f)-N(f_0)]\,L^{\top}(f_0), \tag{22}$$

where

$$N(f)=\int M(f)\,B(f)\,\widetilde{R}^{-1}(f)\,B^{\top}(f)\,M^{\top}(f)\,df. \tag{23}$$

5. Analytical Solution to the Rendezvous Problem

The problem is completely solved if the symmetric matrix $N(f)$ in (23) is obtained analytically. It is convenient to define $r_i = 1/R_i$, $i = 1\ldots3$, and to treat $N(f)$ as the sum of three matrices, corresponding to the weights along the three axes of the rotating frame. Consequently,

$$N(f) = r_1N^{(r)}(f) + r_2N^{(\theta)}(f) + r_3N^{(3)}(f). \tag{24}$$

By virtue of the fact that the in-plane and out-of-plane dynamics are uncoupled, the matrix $N^{(3)}$ only has $N^{(3)}_{5\ldots6,5\ldots6}$ as non-zero elements, and conversely, $N^{(r)}$ and $N^{(\theta)}$ only have $N^{(r)}_{1\ldots4,1\ldots4}$ and $N^{(\theta)}_{1\ldots4,1\ldots4}$ as non-zero elements. Furthermore, derivations reveal that when the in-plane weights are equal, i.e. $R_1 = R_2$, the matrix $N(f)$ is composed of completely closed-form, analytical expressions. This, however, is only a specific case, and excludes all cases where it may be necessary to preferentially use one in-plane control. When $R_1 \neq R_2$, it is observed

that the expressions require the integration of functions whose analytical solutions are not yet known. This problem is explained, and solved, in detail in the next section.

For a more general formulation of the control problem, it is assumed that the weights are unequal, and consequently, it is found useful to rewrite (24) as the following:

$$\begin{aligned} N(f) &= r_1 \left[N^{(r)}(f) + (1-\sigma) N^{(\theta)}(f) \right] + r_3 N^{(3)}(f) \\ &= r_1 \left[N^{(1)}(f) + \sigma N^{(2)}(f) \right] + r_3 N^{(3)}(f), \end{aligned} \tag{25}$$

where,

$$N^{(1)}(f) = N^{(r)}(f) + N^{(\theta)}(f), \quad N^{(2)}(f) = -N^{(\theta)}(f), \quad \sigma = 1 - \frac{r_2}{r_1}. \tag{26}$$

For convenience, the matrices $N^{(1)}$ and $N^{(2)}$ are rewritten as the sum of the following components:

$$N^{(1)} = N^{(13)} E^3 + N^{(12)} E^2 + N^{(11)} E + N^{(10)} \tag{27}$$

$$\begin{aligned} N^{(2)} = {} & N^{(22)} \int E^2 \, df + N^{(21)} \int E \, df + N^{(2c1)} \int E \cos E \, df + N^{(2s1)} \int E \sin E \, df \\ & + N^{(2c2)} \int E \cos 2E \, df + N^{(2s2)} \int E \sin 2E \, df + N^{(20)} \int \frac{dE}{(1 - e \cos E)} \\ & + N^{(20c1)} \int \frac{\cos E \, dE}{(1 - e \cos E)} + N^{(20s1)} \int \frac{\sin E \, dE}{(1 - e \cos E)} \\ & + N^{(20c2)} \int \frac{\cos 2E \, dE}{(1 - e \cos E)} + N^{(20s2)} \int \frac{\sin 2E \, dE}{(1 - e \cos E)} \\ & + N^{(20c3)} \int \frac{\cos 3E \, dE}{(1 - e \cos E)} + N^{(20s3)} \int \frac{\sin 3E \, dE}{(1 - e \cos E)} \end{aligned}$$

$$+N^{(20c4)} \int \frac{\cos 4E \, dE}{(1 - e \cos E)} + N^{(20s4)} \int \frac{\sin 4E \, dE}{(1 - e \cos E)}. \tag{28}$$

For clarity, the superscripts in (28) are used to denote the integral to which the matrices correspond. The matrices $N^{(1\ldots3)}$ can be obtained easily with the aid of a symbolic algebra tool such as Maple®, and are provided as appendices, in terms of the eccentric anomaly, E. Since the matrix N is now known analytically, the cross-component transition matrix, $\Phi_{x\lambda}$ is also known analytically. Consequently, from (15), the initial costates for given initial and final conditions, and initial and final true anomalies, can be determined analytically. If the initial conditions and initial true anomaly are replaced by the current states and current true anomaly, then (15) essentially provides a feedback control law, without the necessity of solving the Riccati equation (Ref. 32) numerically for this system.

The methodology described above can also be extended to the intercept problem, where the final velocity of the chaser is unconstrained. In this case, the final values of the costates corresponding to the velocity components, $\lambda_{4,5,6}(f_T) = 0$. Therefore, the number of boundary conditions is unchanged. The initial values for the costates can still be obtained from the state transition matrix Φ for the Hamiltonian system comprising x and λ; however, the rows require rearrangement to obtain the appropriate block matrices. Consequently, $\Phi_{x\lambda}$ still requires evaluation by the use of the matrix N.

6. General Case of Unequal Weights and Special Integrals

It is observed from (26), that when the in-plane weights are equal, $r_2 = r_1$, and $\sigma = 0$. In this case, the matrix $N^{(2)}$ is not required, and completely closed form solutions are possible. When the in-plane weights are unequal, $\sigma \neq 0$, the matrix $N^{(2)}$ is required, and it can be shown that this requires the following integrals:

$$\int \frac{\cos mE\, dE}{(1 - e\cos E)}, \quad \int \frac{\sin mE\, dE}{(1 - e\cos E)}, \quad m = 1, \ldots, 4. \tag{29}$$

For any $m \geq 0$, the solutions to (29) can be obtained by solving the following integral:

$$I_m = \int \frac{\exp(\imath mE)\, dE}{(1 - e\cos E)} \tag{30}$$

Upon changing the variable of integration to $\chi = \exp(\imath E)$, it can be shown that

$$I_m = \left(\frac{2\imath}{e}\right) \int \frac{\chi^m\, d\chi}{(\chi - \varepsilon)(\chi - 1/\varepsilon)}, \tag{31}$$

$$\varepsilon = \sqrt{(1-\eta)/(1+\eta)}. \tag{32}$$

Decomposing (31) into partial fractions, I_m is solved as follows:

$$I_m = \left(\frac{\imath}{\eta}\right) \left[\int \frac{\chi^m\, d\chi}{(\chi - 1/\varepsilon)} - \int \frac{\chi^k\, d\chi}{(\chi - \varepsilon)}\right] \tag{33}$$

$$= \left(\frac{\imath}{\eta}\right) \left[\sum_{j=0}^{m-1} \frac{1}{\varepsilon^{m-j-1}} \frac{\chi^{j+1}}{(j+1)} + \frac{1}{\varepsilon^m} \ln(\chi - 1/\varepsilon) - \sum_{j=0}^{m-1} \varepsilon^{m-j-1} \frac{\chi^{j+1}}{(j+1)} - \varepsilon^m \ln(\chi - \varepsilon)\right]. \tag{34}$$

It is readily shown that

$$\chi^{j+1} = \cos(j+1)E + \imath \sin(j+1)E. \tag{35}$$

Some algebra and half-angle formulae can be used to show that

$$\ln(\chi - 1/\varepsilon) = \frac{1}{2}\ln(1 - e\cos E) + \imath\frac{1}{2}(E - f) + \text{const}, \tag{36a}$$

$$\ln(\chi - \varepsilon) = \frac{1}{2}\ln(1 - e\cos E) + \imath\frac{1}{2}(E + f) + \text{const}. \tag{36b}$$

Using (36) in (34) and comparing real and imaginary parts, one obtains

$$\begin{aligned}\int \frac{\cos mE\, dE}{(1 - e\cos E)} &= -\frac{1}{\eta}\sum_{j=0}^{m-1}\frac{\sin(j+1)E}{(j+1)}\left(\frac{1}{\varepsilon^{m-j-1}} - \varepsilon^{m-j-1}\right) \\ &\quad -\frac{E}{2\eta}\left(\frac{1}{\varepsilon^m} - \varepsilon^m\right) + \frac{f}{2\eta}\left(\frac{1}{\varepsilon^m} + \varepsilon^m\right), \end{aligned} \tag{37a}$$

$$\begin{aligned}\int \frac{\sin mE\, dE}{(1 - e\cos E)} &= \frac{1}{\eta}\sum_{j=0}^{m-1}\frac{\cos(j+1)E}{(j+1)}\left(\frac{1}{\varepsilon^{m-j-1}} - \varepsilon^{m-j-1}\right) \\ &\quad +\frac{1}{2\eta}\left(\frac{1}{\varepsilon^m} - \varepsilon^m\right)\ln(1 - e\cos E). \end{aligned} \tag{37b}$$

Closed-form solutions to $\int E\, df$, $\int E^2\, df$, $\int E\sin mE\, df$, $\int E\cos mE\, df$, $(m = 1, 2)$ are not yet known. In this section, series solutions to these indefinite integrals are developed, and their convergence properties are discussed. From (3), it can be shown that

$$\frac{df}{dE} = \frac{\eta}{1 - e\cos E}. \tag{38}$$

Using (37), the following Fourier series in harmonics of the eccentric anomaly can be devel-

oped:

$$\frac{1}{(1-e\cos E)} = \gamma_0 + \sum_{k=1}^{\infty} \gamma_k \cos kE, \tag{39a}$$

$$\gamma_0 = \frac{1}{2\pi}\left(I_0\Big|_{E=2\pi,f=2\pi} - I_0\Big|_{E=0,f=0}\right) = \frac{1}{\eta}, \tag{39b}$$

$$\gamma_k = \frac{1}{\pi}\left(I_k\Big|_{E=2\pi,f=2\pi} - I_k\Big|_{E=0,f=0}\right) = \frac{2\varepsilon^k}{\eta}. \tag{39c}$$

It follows that (38) may be rewritten as

$$df = \left[1 + 2\sum_{k=1}^{\infty} \varepsilon^k \cos kE\right] dE. \tag{40}$$

Consequently, it can be shown that

$$\int E\, df = Ef - \frac{E^2}{2} + 2\sum_{k=1}^{\infty} \frac{\varepsilon^k}{k^2}\cos kE, \tag{41a}$$

$$\int E^2\, df = E^2 f - \frac{2E^3}{3} + 4E\sum_{k=1}^{\infty} \frac{\varepsilon^k}{k^2}\cos kE - 4\sum_{k=1}^{\infty} \frac{\varepsilon^k}{k^3}\sin kE, \tag{41b}$$

$$\begin{aligned}\int E\sin E\, df &= \frac{2\eta}{e}\sum_{k=1}^{\infty} \frac{\varepsilon^k}{k^2}\sin kE - \frac{2\eta}{e}E\sum_{k=1}^{\infty} \frac{\varepsilon^k}{k}\cos kE \\ &= \frac{\eta}{e}E\ln\left[\frac{2(1-e\cos E)}{(1+\eta)}\right] + \frac{2\eta}{e}\sum_{k=1}^{\infty} \frac{\varepsilon^k}{k^2}\sin kE,\end{aligned} \tag{41c}$$

$$\int E\cos E\, df = \frac{\varepsilon}{2}E^2 + \frac{1}{e}E(f-E) + \frac{2}{e}\sum_{k=1}^{\infty} \frac{\varepsilon^k}{k^2}\cos kE, \tag{41d}$$

$$\begin{aligned}\int E\sin 2E\, df &= \frac{2\eta}{e^2}E\ln\left[\frac{2(1-e\cos E)}{(1+\eta)}\right] - \frac{2\eta}{e}\left(\sin E - E\cos E\right) \\ &\quad + \frac{4\eta}{e^2}\sum_{k=1}^{\infty} \frac{\varepsilon^k}{k^2}\sin kE,\end{aligned} \tag{41e}$$

$$\int E\cos 2E\,df = \frac{\varepsilon^2}{2}E^2 + \frac{(2-e^2)}{e^2}E(f-E) - \frac{2\eta}{e}\left(\cos E + E\sin E\right) + \frac{2(2-e^2)}{e^2}\sum_{k=1}^{\infty}\frac{\varepsilon^k}{k^2}\cos kE. \tag{41f}$$

In the above equations, the arbitrary constants of integration have been ignored since these equations are evaluated with lower limit f_0 and upper limit f_T (E_0 and E_T, respectively).

Although (41) are composed of convergent infinite series for all values of $e < 1$, in practice, not all terms are required for computation. The series depend on a parameter $\varepsilon < 1$, and beyond a certain value of $k = k_{\max}$, the contribution of higher-order terms will be numerically insignificant. Therefore, the series may be truncated at the prescribed value $k_{\max}$, which can be derived by studying the convergence properties of the following general expression:

$$q\sum_{k=1}^{\infty}\frac{\varepsilon^k}{k^p}\exp(\imath kE) \tag{42}$$

where $p \in \mathbb{Z}_{>0}$ and $q \in \mathbb{R}$.

A value for $k_{\max}$ is sought such that terms in the above series where $k > k_{\max}$ contribute less than $10^{-N_{\text{tol}}}$, where N_{tol} is a number denoting the desired numerical tolerance within which the truncated series representation must agree with the (unknown) true solution. This tolerance can be chosen to satisfy any requirement. For example, suitable choices for N_{tol} are the tolerance used to solve Kepler's equation numerically, or the tolerance employed for

numerical integration. This requirement is represented by the following inequality:

$$\left| q \sum_{k=k^*}^{\infty} \frac{\varepsilon^k}{k^p} \exp(\imath k E) \right| \leq 10^{-N_{\text{tol}}}, \tag{43}$$

where

$$k^* = k_{\max} + 1. \tag{44}$$

It is easily observed that:

$$\left| q \sum_{k=k^*}^{\infty} \frac{\varepsilon^k}{k^p} \exp(\imath k E) \right| \leq |q| \sum_{k=k^*}^{\infty} \frac{\varepsilon^k}{k^p}. \tag{45}$$

The following inequality is developed for the sum on the right hand side of (45):

$$\begin{aligned} |q| \sum_{k=k^*}^{\infty} \frac{\varepsilon^k}{k^p} &= |q|\, \varepsilon^{k^*} \left[\frac{1}{k^{*p}} + \frac{\varepsilon}{(k^*+1)^p} + \frac{\varepsilon^2}{(k^*+2)^p} + \cdots \right] \\ &\leq |q|\, \varepsilon^{k^*} \left[\frac{1}{k^{*p}} + \frac{\varepsilon}{k^{*p}} + \frac{\varepsilon^2}{k^{*p}} + \cdots \right] \\ &= \frac{|q|}{(1-\varepsilon)} \frac{\varepsilon^{k^*}}{k^{*p}}. \end{aligned} \tag{46}$$

Consequently, a solution to the following equation is desired:

$$\frac{|q|}{(1-\varepsilon)} \frac{\varepsilon^{k^*}}{k^{*p}} = 10^{-N_{\text{tol}}}, \tag{47}$$

or,

$$c_e k^* + p \ln k^* = c_N, \tag{48}$$

where,

$$c_e = -\log \varepsilon, \quad c_N = N_{\text{tol}} \log 10 + \log |q| - \log(1-\varepsilon). \tag{49}$$

Equation (48) is rewritten as the following:

$$\bar{k} \, \exp(\bar{k}) = \frac{c_e}{p} \exp\left(\frac{c_N}{p}\right), \tag{50}$$

where $\bar{k} = (c_e/p)\, k^*$. Equation (50) yields the following solutions for $k_{\max}$:

$$k_{\max} = \lceil k^* \rceil - 1 = \begin{cases} \lceil \, (c_N/c_\varepsilon) \, \rceil - 1, & p = 0 \\ \\ \left\lceil \, (p/c_e) \, \mathcal{W}\Big(\exp\left(c_N/p\right) \, c_e/p \Big) \, \right\rceil - 1, & p > 0 \end{cases}, \tag{51}$$

where $\lceil \cdot \rceil$ is the ceiling operator that denotes the smallest integer larger than the argument, and $\mathcal{W}$ denotes the Lambert W function (Ref. 33). Although efficient methods exist to evaluate the Lambert W function (Ref. 34), a second-order Newton-Raphson solution, that is correct for $q = 1$, $p \leq 3$, $N_{\text{tol}} \leq 15$, and $e \leq 0.99$, is given by the following:

$$k_{\max} = \left\lceil \frac{c_N}{c_e} \left\{ 1 - \frac{2p \, (c_N + p) \log \left(c_N/c_e\right)}{[2(c_N+p)^2 + p^2 \log \left(c_N/c_e\right)]} \right\} \right\rceil - 1. \tag{52}$$

Figure 1 shows the number of terms at which the infinite series with $p = 2$, may be terminated, for tolerance values of $N_{\text{tol}} = 9$ (solid), $N_{\text{tol}} = 12$ (dashed), and $N_{\text{tol}} = 15$ (dotted). It is observed that $k_{\max}$ rises drastically, beyond an eccentricity of $e = 0.9$. However, it is worth noting first, that this is only a matter of concern when the in-plane weights are unequal.

Second, as noted earlier, at high values of eccentricity, the dynamics of the problem are perturbed greatly by nonlinearity effects (Ref. 31), and an optimal control based on linear analysis is no longer sufficient even for small relative distances. Third, it is easy to generate higher-order terms from lower-order terms recursively. For example,

$$\cos(k+1)E = \cos kE\,\cos E - \sin kE\,\sin E, \tag{53a}$$

$$\frac{\varepsilon^{k+1}}{(k+1)^2} = \frac{\varepsilon}{(1+k^{-1})^2}\cdot\frac{\varepsilon^k}{k^2}. \tag{53b}$$

Fourth, the series representations only require evaluation at the initial and final values of true or eccentric anomaly, and do not require numerical integration. Finally, even though the number of terms required may be large, $k_{\max}$ is known *a priori*, and no convergence tests or arbitrarily large choices are required. Accuracy may be sacrificed for a reduction of the number of terms; for example, it is still possible to obtain an accuracy of 10^{-9} at $e = 0.95$ with 40 terms in the series, instead of an accuracy of 10^{-15} using 80 terms.

7. Numerical Simulations

In this section, the analytical results are compared with the numerical solution to the two-point boundary value problem given by (15), for three sets of weights:

(i) $R_1 = R_2 = R_3 = 1$,

(ii) $R_1 = 100$, $R_2 = R_3 = 1$,

(iii) $R_1 = \infty$, $R_2 = R_3 = 1$.

All examples assume a target orbit eccentricity of $e = 0.4$, and use the following initial and final conditions:

$$f_0 = 0.61087, \quad x_0 = \{0\ 1\ 0\ 0.5\ 0\ 1\}^\top, \tag{54a}$$

$$f_T = 20.71705, \quad x_T = \{1\ 0\ 2\ 0\ -1.71429\ 0\}^\top. \tag{54b}$$

The difference between the final and initial true anomalies corresponds to approximately three revolutions of the target about the Earth, in its orbit. It is worth noting that as f_T increases, the amount of time taken by numerical integration employed by shooting methods, also increases.

It is first assumed that $R_1 = R_2 = R_3 = 1$. Since $\sigma = 0$, it is not necessary to evaluate the matrix $N^{(2)}$ or the series given by (41). Upon evaluating the matrices in the appendix, $\overline{N}$ is calculated, and the initial costate vector is as follows:

$$\lambda_{01} = \{0.19338\ -0.00317\ -0.02156\ 0.02658\ 0.10683\ -0.03163\}^\top. \tag{55}$$

In the second case, it is assumed that $R_1 = 100$, $R_2 = R_3 = 1$; that is, the control law penalizes the use of radial thrust. In this case the series solutions to evaluate $N^{(2)}$ are made use of. It is assumed that the series solution is truncated to only as many terms as

are required to guarantee an accuracy of 10^{-14}. The particular choice of $e = 0.4$ results in $\eta = 0.91652$ and $\varepsilon = 0.20871$. Using these values of η and ε, and $N_{\text{tol}} = 14$ in either (51) or (52) provides the following values for the number of terms required in the series:

$$p = 2, k_{\max} = 17; \quad p = 3, k_{\max} = 15. \tag{56}$$

Therefore, the series used to calculate the matrix $N^{(2)}$ may be restricted to 17 terms only. The advantage of the formulation in this paper is immediately obvious in the fact that the required number of terms can be calculated at any stage of the maneuver, only requires the desired tolerance and eccentricity of the target orbit, does not depend on the relative trajectory or boundary conditions, and does not require numerical integration.

Using the set of weights as specified above, the initial costates are obtained as follows:

$$\lambda_{02} = \{0.25136 \ -0.00326 \ -0.02156 \ 0.02853 \ 0.11908 \ -0.03163\}^{\top}. \tag{57}$$

Finally, the radial control effort is completely removed by choosing $R_1 = \infty$, $R_2 = R_3 = 1$. Numerically, this is performed by choosing $r_3 = 1$, $r_1 = 0$, but $r_1\sigma = 1$, in (25) and (26), which results in $r_2 = 1$. The initial costates for this case are given by:

$$\lambda_{03} = \{0.21560 \ -0.00326 \ -0.02156 \ 0.02855 \ 0.11921 \ -0.03163\}^{\top}. \tag{58}$$

The values of λ_{01}, λ_{02}, λ_{03} obtained by solving the two-point boundary value problem agree with (55)-(58) respectively, within the tolerance of 10^{-12} prescribed for numerical integration. Numerical simulations for the three cases are shown graphically by Fig. 2, Fig. 3, and Fig. 4. In all three figures, the solid line depicts the case with equal weights ($R_1 = R_2 = R_3 = 1$), the dashed line depicts the case with penalized radial control ($R_1 = 100$, $R_2 = R_3 = 1$), and the dotted line depicts the case with no radial control. The relative trajectory is shown in Fig. 2, where the circle and square are used to show the initial and final relative position. Penalizing the radial control changes the optimal trajectory, from the solid line (equal weights) to the dashed line (unequal weights). But turning off the radial control effort completely, the dotted line is obtained, and it is observed that the trajectory is nearly the same as that obtained by unequal weights. In all three cases, the boundary conditions are satisfied.

From Fig. 3, the use of $R_1 = 100$ reduces the magnitude of radial control effort to approximately 10^{-4} (dashed line), which is three orders of magnitude lower than the along-track or out-of-plane control effort. The use of $R_1 = \infty$ results in a magnitude of radial control effort of exactly zero, as shown by the dotted line, although this is indistinguishable from the second case, given the scale of the figure. The along-track control history differs for all three cases, because this control has to compensate for the cases where the magnitude of

the radial control effort is reduced by unequal weights (dashed line), or zero radial control effort (dotted line). The variation of along-track control is indistinguishable in the last two cases. The out-of-plane control effort is identical in all three cases, as is easily evident from the fact that the third and sixth components of the initial costate vectors given by (55)-(58), are equal.

The cost for rendezvous, $\mathcal{J}_{\text{fuel}}$, is calculated from (10), and is shown in Fig. 4. Penalizing the radial control effort only increases the total cost slightly, as can be observed by comparing the dashed line with the solid line. Forcing the radial control effort to zero, as shown by the dotted line, does not result in a change in cost that is visible on the scale.

8. Conclusions

In this paper, the problem of power-limited, continuous-thrust optimal rendezvous near elliptic orbits in a central field, has been solved analytically. The general case of unequal weights for radial, along-track, and out-of-plane thrusts, requires the evaluation of several integrals whose solutions are best represented by series in a small eccentricity-dependent parameter, and it is shown that these series may be truncated effectively within any numerical precision desired. The use of unequal weights also demonstrates how penalizing the radial control effort results in an optimal control law using along-track and out-of-plane thrusts only. Since the costates can be determined without integration or numerical methods, for

any given initial and final conditions, the theory is also sufficient to design effective optimal feedback controls, or for receding horizon control. The number of operations are limited to the evaluation of the eccentric and true anomalies from the current time, the sines and cosines of the anomalies, the evaluation of the number of terms from the Lambert W function or its approximation, and the evaluation of the matrices in the appendices. This number is far smaller than the number of operations required for numerical integration and numerical solution to a two-point boundary value problem for the linear rendezvous problem. Finally, the initial costate values determined analytically, can serve as suitable initial guesses for iterative numerical procedures used to solve the nonlinear rendezvous problem.

Appendix A: Matrices $N^{(1)}$ and $N^{(3)}$ ($R_1 = R_2$)

The nonzero components of the symmetric matrices, $N^{(13)}$, $N^{(12)}$, $N^{(11)}$, and $N^{(10)}$, in terms of the eccentric anomaly, E, are given as follows:

$$N_{44}^{(13)} = \frac{3}{\eta^{11}},\ N_{24}^{(13)} = eN_{44}^{(13)},\ N_{22}^{(13)} = eN_{24}^{(13)},$$

$$N_{34}^{(12)} = \frac{3}{2\eta^{6}},\ N_{23}^{(12)} = eN_{34}^{(12)},\ N_{44}^{(12)} = \frac{9e}{\eta^{11}}\sin E,\ N_{24}^{(12)} = eN_{44}^{(12)},\ N_{22}^{(12)} = eN_{24}^{(12)},$$

$$N_{11}^{(11)} = \frac{5}{2\eta^{7}},\ N_{14}^{(11)} = -\frac{6}{\eta^{8}}\sin E,\ N_{12}^{(11)} = eN_{14}^{(11)},\ N_{34}^{(11)} = -\frac{e\eta^{2}}{2}N_{14}^{(11)},\ N_{23}^{(11)} = eN_{34}^{(11)},$$

$$N_{22}^{(11)} = \frac{3e^4}{2\eta^{11}}\cos 2E + \frac{12e(1+3e^2)}{\eta^{11}}\cos E + \frac{1}{2\eta^{11}}(5+23e^2+13e^4),$$

$$N_{24}^{(11)} = \frac{3e^3}{2\eta^{11}}\cos 2E + \frac{6(1+8e^2-e^4)}{\eta^{11}}\cos E + \frac{e}{2\eta^{11}}(25+24e^2-8e^4),$$

$$N_{33}^{(11)} = \frac{1}{\eta},$$

$$N_{44}^{(11)} = \frac{3e^2}{2\eta^{11}}\cos 2E + \frac{12e(5-e^2)}{\eta^{11}}\cos E + \frac{1}{2\eta^{11}}(8+62e^2-33e^4+4e^6),$$

$$\begin{aligned}
N_{11}^{(10)} &= -\frac{e}{12\eta^7}\sin 3E + \frac{3}{4\eta^7}\sin 2E - \frac{15e}{4\eta^7}\sin E,\\
N_{12}^{(10)} &= \frac{e}{12\eta^8}\cos 3E - \frac{3(1+e^2)}{4\eta^8}\cos 2E - \frac{27e}{4\eta^8}\cos E,\\
N_{13}^{(10)} &= -\frac{2}{\eta^3}\sin E,\\
N_{14}^{(10)} &= \frac{e^2}{12\eta^8}\cos 3E - \frac{e(7-e^2)}{4\eta^8}\cos 2E - \frac{(32-5e^2)}{4\eta^8}\cos E,\\
N_{22}^{(10)} &= \frac{e(1-e^2-e^4)}{12\eta^{11}}\sin 3E - \frac{3(1+e^2+2e^4)}{4\eta^{11}}\sin 2E - \frac{3e(23+61e^2+e^4)}{4\eta^{11}}\sin E,\\
N_{23}^{(10)} &= \frac{e^3}{4\eta^6}\cos 2E + \frac{2(1+3e^2)}{\eta^6}\cos E,\\
N_{24}^{(10)} &= \frac{e^2(1-2e^2)}{12\eta^{11}}\sin 3E - \frac{e(7+7e^2-2e^4)}{4\eta^{11}}\sin 2E - \frac{(32+253e^2-26e^4-4e^6)}{4\eta^{11}}\sin E,\\
N_{33}^{(10)} &= \frac{e}{\eta}\sin E,\\
N_{34}^{(10)} &= \frac{e^2}{4\eta^6}\cos 2E + \frac{2e(5-e^2)}{\eta^6}\cos E,\\
N_{44}^{(10)} &= -\frac{e^5}{12\eta^{11}}\sin 3E - \frac{e^2(23-13e^2+2e^4)}{4\eta^{11}}\sin 2E - \frac{e(304-28e^2-25e^4+4e^6)}{4\eta^{11}}\sin E.
\end{aligned}$$

The nonzero components of the symmetric matrix $N^{(3)}$, in terms of the eccentric anomaly,

are given as follows:

$$
\begin{aligned}
N_{55}^{(3)} &= \frac{1}{2\eta^5}E + \frac{e}{12\eta^5}\sin 3E - \frac{1}{4\eta^5}\sin 2E - \frac{e}{4\eta^5}\sin E, \\
N_{56}^{(3)} &= \frac{e}{12\eta^6}\cos 3E - \frac{(1+e^2)}{4\eta^6}\cos 2E + \frac{5e}{4\eta^6}\cos E, \\
N_{66}^{(3)} &= \frac{(1+4e^2)}{2\eta^7}E - \frac{e}{12\eta^7}\sin 3E + \frac{(1+2e^2)}{4\eta^7}\sin 2E - \frac{e(11+4e^2)}{4\eta^7}\sin E.
\end{aligned}
$$

Appendix B: Matrix $N^{(2)}$ $(R_1 \neq R_2)$

The nonzero components of the symmetric matrices used to evaluate $N^{(2)}$ are shown below:

$$N_{44}^{(22)} = -\frac{9}{\eta^{10}},\ N_{24}^{(22)} = eN_{44}^{(22)},\ N_{22}^{(22)} = eN_{24}^{(22)},$$

$$N_{34}^{(21)} = -\frac{3}{\eta^5},\ N_{23}^{(21)} = eN_{34}^{(21)},\ N_{14}^{(21)} = \frac{3}{2\eta^4}N_{23}^{(21)},\ N_{12}^{(21)} = eN_{14}^{(21)},$$

$$N_{14}^{(2c1)} = \frac{6}{\eta^9},\ N_{12}^{(2c1)} = eN_{14}^{(2c1)},$$

$$N_{22}^{(2s1)} = \frac{12e(1+e^2)}{\eta^{10}},\ N_{24}^{(2s1)} = \frac{3(2+7e^2-e^4)}{\eta^{10}},\ N_{44}^{(2s1)} = \frac{6e(5-e^2)}{\eta^{10}},$$

$$N_{14}^{(2c2)} = -\frac{3e}{2\eta^9},\ N_{12}^{(2c2)} = eN_{14}^{(2c1)},$$

$$N_{24}^{(2s2)} = -\frac{3e(1+e^2)}{2\eta^{10}},\ N_{44}^{(2s2)} = -\frac{3e^2}{\eta^{10}},\ N_{22}^{(2s2)} = N_{44}^{(2s2)},$$

$$N_{11}^{(20)}=-\frac{(16+19e^2)}{8\eta^7},\ N_{13}^{(20)}=-\frac{3}{2\eta^3},\ N_{22}^{(20)}=-\frac{(16+33e^2+16e^4)}{8\eta^9},,$$
$$N_{24}^{(20)}=-\frac{e(40+33e^2-8e^4)}{8\eta^9},\ N_{33}^{(20)}=-\eta,\ N_{44}^{(20)}=-\frac{e^2(100-39e^2+4e^4)}{8\eta^9},$$

$$N_{11}^{(20c1)}=\frac{7e}{\eta^7},\ N_{13}^{(20c1)}=\frac{2}{\eta^3},\ N_{22}^{(20c1)}=\frac{e(1+e^2)}{\eta^9},\ N_{24}^{(20c1)}=\frac{e^2(7+e^2)}{4\eta^9},\ N_{44}^{(20c1)}=\frac{e^3(5-e^2)}{2\eta^9},$$

$$N_{12}^{(20s1)}=\frac{e(6+5e^2)}{2\eta^8},\ N_{14}^{(20s1)}=\frac{e^2(27-5e^2)}{4\eta^8},\ N_{23}^{(20s1)}=\frac{2(1+e^2)}{\eta^4},\ N_{34}^{(20s1)}=\frac{e(5-e^2)}{\eta^4},$$

$$N_{11}^{(20c2)}=-\frac{(4+3e^2)}{2\eta^7},\ N_{13}^{(20c2)}=-\frac{e}{2\eta^3},\ N_{22}^{(20c2)}=\frac{2(1+e^2)^2}{\eta^9},,$$
$$N_{24}^{(20c2)}=\frac{e(1+e^2)(5-e^2)}{\eta^9},\ N_{44}^{(20c2)}=\frac{e^2(5-e^2)^2}{2\eta^9},$$

$$N_{12}^{(20s2)}=-\frac{(8+11e^2)}{4\eta^8},\ N_{14}^{(20s2)}=-\frac{e(20-e^2)}{4\eta^8},\ N_{23}^{(20s2)}=-\frac{e}{2\eta^4},\ N_{34}^{(20s2)}=eN_{23}^{(20s2)},$$

$$N_{11}^{(20c3)}=\frac{e}{\eta^7},\ N_{22}^{(20c3)}=-\frac{e(1+e^2)}{\eta^9},\ N_{24}^{(20c3)}=-\frac{e^2(7+e^2)}{4\eta^9},\ N_{44}^{(20c3)}=-\frac{e^3(5-e^2)}{2\eta^9},$$

$$N_{12}^{(20s3)}=\frac{e(2+e^2)}{2\eta^8},\ N_{14}^{(20s3)}=\frac{e^2(7-e^2)}{4\eta^8},$$

$$N_{11}^{(20c4)}=-\frac{e^2}{8\eta^7},\ N_{22}^{(20c4)}=-\frac{1}{\eta^2}N_{11}^{(20c4)},\ N_{24}^{(20c4)}=eN_{22}^{(20c4)},\ N_{44}^{(20c4)}=eN_{24}^{(20c4)},$$

$$N_{12}^{(20s4)}=-\frac{e^2}{8\eta^8},\ N_{14}^{(20s4)}=eN_{12}^{(20s4)}.$$

References

1. HILL, G. W., *Researches in the Lunar Theory*, American Journal of Mathematics, Vol. 1, No. 1, pp. 5–26, 1878.

2. CLOHESSY, W. H., and WILTSHIRE, R. S., *Terminal Guidance System for Satellite Rendezvous*, Journal of the Aerospace Sciences, Vol. 27, pp. 653–658, 674, 1960.

3. TSCHAUNER, J. F. A., and HEMPEL, P. R., *Rendezvous zu einemin Elliptischer Bahn umlaufenden Ziel*, Astronautica Acta, Vol. 11, No. 2, pp. 104–109, 1965.

4. CARTER, T. E., and HUMI, M., *Fuel-Optimal Rendezvous Near a Point in General Keplerian Orbit*, Journal of Guidance, Control, and Dynamics, Vol. 10, No. 6, pp. 567–573, 1987.

5. CARTER, T. E., *New Form for the Optimal Rendezvous Equations Near a Keplerian Orbit*, Journal of Guidance, Control, and Dynamics, Vol. 13, No. 1, pp. 183–186, 1990.

6. CARTER, T. E., *State Transition Matrices for Terminal Rendezvous Studies: Brief Survey and New Examples*, Journal of Guidance, Control, and Dynamics, Vol. 21, No. 1, pp. 148–155, 1998.

7. YAMANAKA, K., and ANKERSEN, F., *New State Transition Matrix for Relative Motion on an Arbitrary Elliptical Orbit*, Journal of Guidance, Control, and Dynamics,

Vol. 25, No. 1, pp. 60–66, 2002.

8. LAWDEN, D. F., *Optimal Trajectories for Space Navigation*, Butterworths, London, UK, 1963, 2nd ed.

9. BILLIK, B. H., *Some Optimal Low-Acceleration Rendezvous Maneuvers*, AIAA Journal, Vol. 2, No. 3, pp. 510–516, 1964.

10. EDELBAUM, T. N., *Optimum Low-Thrust Rendezvous and Stationkeeping*, AIAA Journal, Vol. 2, No. 7, pp. 1196–1201, 1964.

11. GOBETZ, F. W., *Linear Theory of Optimum Low-Thrust Rendezvous Trajectories*, The Journal of the Astronautical Sciences, Vol. 12, No. 3, pp. 69–76, 1965.

12. ALFRIEND, K. T., and KASHIWAGI, Y., *Minimum Time Optimal Rendezvous Between Neighboring Elliptic Orbits*, Journal of Optimization Theory and Applications, Vol. 4, No. 4, pp. 260–276, 1969.

13. JEZEWSKI, D. J., and STOOLZ, J. M., *A Closed-form Solution for Minimum-Fuel, Constant-Thrust Trajectories*, AIAA Journal, Vol. 8, No. 7, pp. 1229–1234, 1970.

14. CARTER, T. E., and BRIENT, J., *Fuel-Optimal Rendezvous for Linearized Equations of Motion*, Journal of Guidance, Control, and Dynamics, Vol. 15, No. 6, pp. 1411–1416, 1992.

15. HUMI, M., *Fuel-Optimal Rendezvous in a General Central Gravity Field*, Journal of

Guidance, Control, and Dynamics, Vol. 16, No. 1, pp. 215–217, 1993.

16. CARTER, T. E., and BRIENT, J., *Linearized Impulsive Rendezvous Problem*, Journal of Optimization Theory and Applications, Vol. 86, No. 3, pp. 553–584, 1995.

17. INALHAN, G., TILLERSON, M., and HOW, J. P., *Relative Dynamics and Control of Spacecraft Formations in Eccentric Orbits*, Journal of Guidance, Control, and Dynamics, Vol. 25, No. 1, pp. 48–59, 2002.

18. EULER, E. A., *Optimal Low-Thrust Rendezvous Control*, AIAA Journal, Vol. 7, No. 6, pp. 1140–1144, 1969.

19. CARTER, T. E., and BRIENT, J., *Optimal Bounded-Thrust Space Trajectories Based on Linearized Equations*, Journal of Optimization Theory and Applications, Vol. 70, No. 2, pp. 299–317, 1991.

20. CARTER, T. E., *Optimal Power-Limited Rendezvous for Linearized Equations of Motion*, Journal of Guidance, Control, and Dynamics, Vol. 17, No. 5, pp. 1082–1086, 1994.

21. COVERSTONE-CARROLL, V. L., and PRUSSING, J. E., *Optimal Cooperative Power-Limited Rendezvous Between Neighboring Circular Orbits*, Journal of Guidance, Control, and Dynamics, Vol. 16, No. 6, pp. 1045–1054, 1993.

22. ZANON, D. J., and CAMPBELL, M. E., *Optimal Planner for Spacecraft Formations in Elliptical Orbits*, Journal of Guidance, Control, and Dynamics, Vol. 29, No. 1, pp.

161–171, 2006.

23. SENGUPTA, P., *Comment on "Optimal Planner for Spacecraft Formations in Elliptical Orbits"*, Journal of Guidance, Control, and Dynamics, Vol. 29, No. 6, pp. 1484–1485, 2006.

24. BATTIN, R. H., *An Introduction to the Mathematics and Methods of Astrodynamics*, AIAA Education Series, American Institute of Aeronautics and Astronautics, Inc., Reston, VA, 1999, revised ed.

25. BROUCKE, R. A., *Solution of the Elliptic Rendezvous Problem with the Time as Independent Variable*, Journal of Guidance, Control, and Dynamics, Vol. 26, No. 4, pp. 615–621, 2003.

26. MELTON, R. G., *Time Explicit Representation of Relative Motion Between Elliptical Orbits*, Journal of Guidance, Control, and Dynamics, Vol. 23, No. 4, pp. 604–610, 2000.

27. GIM, D.-W., and ALFRIEND, K. T., *State Transition Matrix of Relative Motion for the Perturbed Noncircular Reference*, Journal of Guidance, Control, and Dynamics, Vol. 26, No. 6, pp. 956–971, 2003.

28. MAREC, J.-P., *Optimal Spacecraft Trajectories*, Vol. 1 of *Studies in Astronautics*, Elsevier Scientific Publishing Company, The Netherlands, 1979.

29. CHANG-DíAZ, F. R., HSU, M. M., BRADEN, E. M., JOHNSON, I. L., and YANG, T.-

F., *Rapid Mars Transits with Exhaust-Modulated Plasma Propulsion*, Tech. Rep. 3539, NASA, 1995.

30. STARIN, S. R., YEDAVALLI, R. K., and SPARKS, A. G., *Spacecraft Formation Flying Maneuvers Using Linear Quadratic Regulation with No Radial Axis Inputs*, *AIAA Guidance, Navigation and Control Conference and Exhibit*, AIAA-2001-4029, AIAA, Montreal, Canada, 2001.

31. SENGUPTA, P., SHARMA, R., and VADALI, S. R., *Periodic Relative Motion Near a Keplerian Elliptic Orbit with Nonlinear Differential Gravity*, Journal of Guidance, Control, and Dynamics, Vol. 29, No. 5, pp. 1110–1121, 2006.

32. LEWIS, F. L., and SYRMOS, V. L., *Optimal Control*, John Wiley & Sons, Inc., New York, NY, 1995, 2nd ed.

33. CORLESS, R. M., GONNET, G. H., HARE, D. E. G., JEFFREY, D. J., and KNUTH, D. E., *On the Lambert W Function*, Advances in Computational Mathematics, Vol. 5, No. 1, pp. 329–359, 1996.

34. CORLESS, R. M., JEFFREY, D. J., and KNUTH, D. E., *A Sequence of Series for the Lambert W Function*, *ISSAC '97: Proceedings of the 1997 International Symposium on Symbolic and Algebraic Computation*, ACM Press, New York, NY, 1997, pp. 197–204.

List of Figure Captions

Figure 1: Variation of Number of Terms Required for Convergence ($k_{\max}$) with Target Orbit Eccentricity (e)

Figure 2: Unscaled Relative Trajectory in LVLH Frame, Equal Weights (Solid), Unequal Weights (Dashed), $R_1 = \infty$ (Dotted)

Figure 3: Optimal Control History Variation with Elapsed Time, Equal Weights (Solid), Unequal Weights (Dashed), $R_1 = \infty$ (Dotted)

Figure 4: Fuel Cost, Equal Weights (Solid), Unequal Weights (Dashed), $R_1 = \infty$ (Dotted)

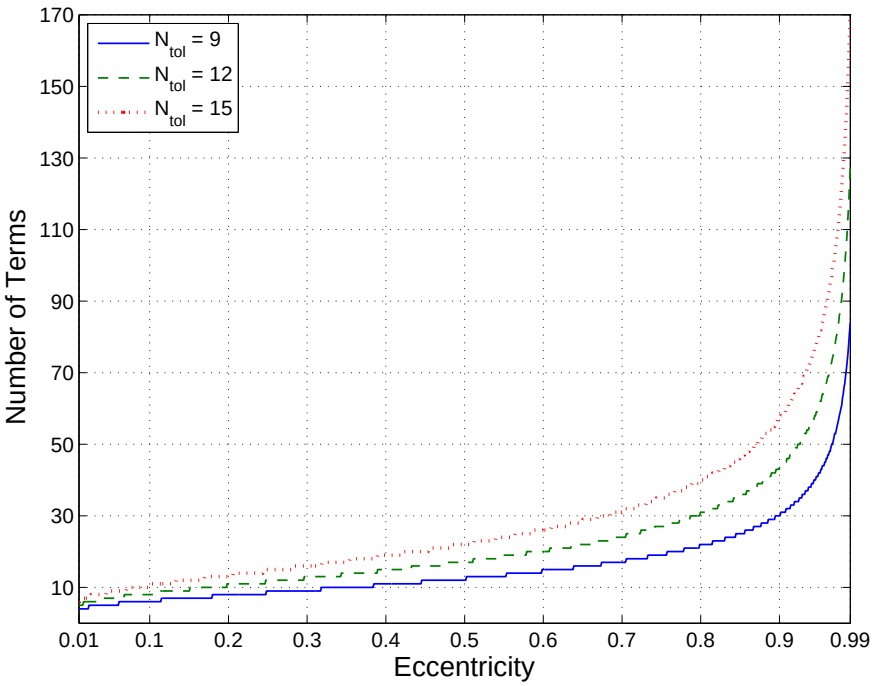
170
150
130
110
90
70
50
30
10
Number of Terms
0.01
0.1
0.2
0.3
0.4
0.5
0.6
0.7
0.8
0.9
0.99
Eccentricity
N_tol = 9
N_tol = 12
N_tol = 15

FIGURE 1:

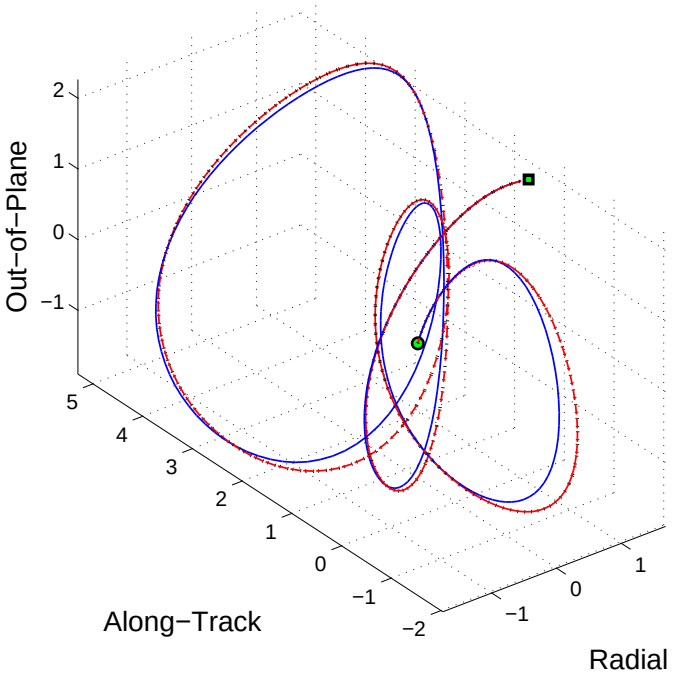

FIGURE 2:

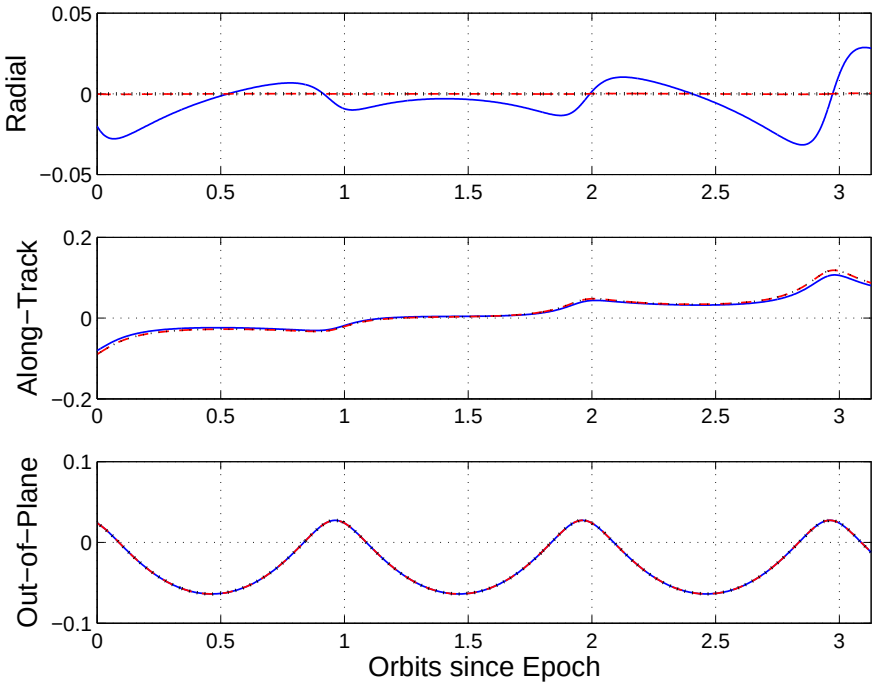
Radial
0.05
0
−0.05
Along−Track
0.2
0
−0.2
Out−of−Plane
0.1
0
−0.1
0
0.5
1
1.5
2
2.5
3
Orbits since Epoch

FIGURE 3:

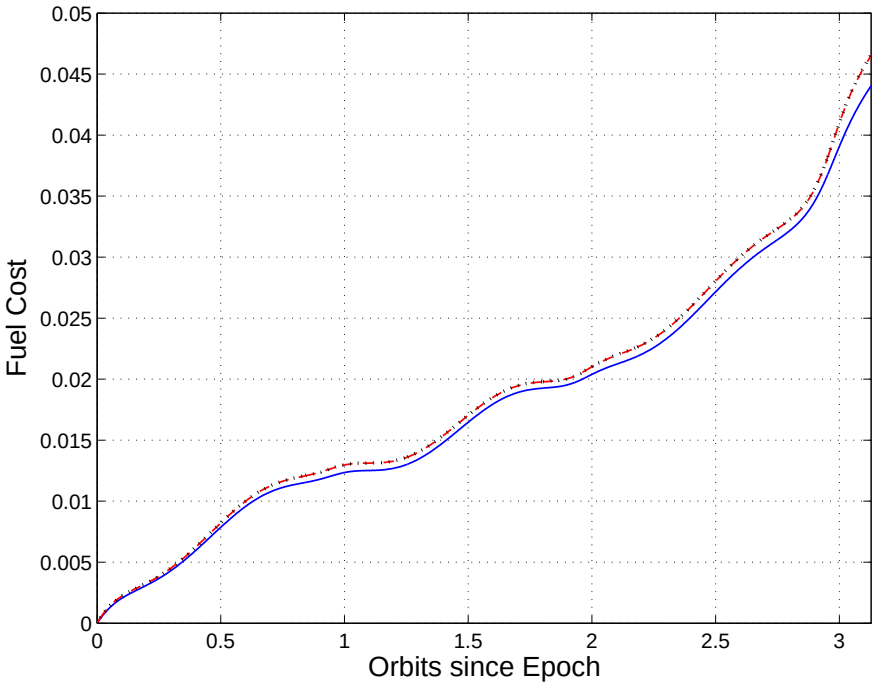
Fuel Cost
Orbits since Epoch
0
0.005
0.01
0.015
0.02
0.025
0.03
0.035
0.04
0.045
0.05
0
0.5
1
1.5
2
2.5
3

FIGURE 4: